

Phys. (Kyoto) 19, 597 (1958).

<sup>2</sup>N. M. Hugenholtz and L. Van Hove, *Physica* 24, 363 (1958).

<sup>3</sup>P. W. Anderson, *Phys. Rev.* 112, 1900 (1958).

<sup>4</sup>D. J. Thouless, *Phys. Rev.* 117, 1256 (1960).

<sup>5</sup>L. N. Cooper, *Phys. Rev.* 122, 1021 (1961).

<sup>6</sup>B. Stölan and L. N. Cooper, *Phys. Rev.* 143, 209 (1966).

<sup>7</sup>N. M. Hugenholtz, *Physica* 23, 481 (1957); in *The Many-Body Problem*, edited by C. Dewitt and P. Nozières (Wiley, New York, 1959), p. 1.

<sup>8</sup>L. Van Hove, *Physica* 21, 901 (1955); 22, 343 (1956).

<sup>9</sup>G. C. Wick, *Phys. Rev.* 80, 268 (1950).

<sup>10</sup>E. C. Titchmarch, *The Theory of Functions*, 2nd ed. (Oxford U. P., Oxford, England, 1939), p. 250.

<sup>11</sup>J. Goldstone, *Proc. Roy. Soc. (London)* A239, 267 (1957).

<sup>12</sup>K. Fukushima and N. Fukuda, *Progr. Theoret. Phys.* (Kyoto) 28, 809 (1962).

<sup>13</sup>H. P. Kelly, *Phys. Rev.* 131, 684 (1963).

<sup>14</sup>M. Gaudin, *Nucl. Phys.* 20, 513 (1960).

PHYSICAL REVIEW B

VOLUME 4, NUMBER 3

1 AUGUST 1971

## Spin-Orbit Coupling and Nuclear Magnetic Resonance in Superconducting Metals\*

W. A. Hines<sup>†</sup> and W. D. Knight

*Department of Physics, University of California, Berkeley, California 94720*

(Received May 14 1970)

In this work, the effect of spin-orbit coupling (through spin-reversing scattering) on the paramagnetic spin susceptibility of conduction electrons in a superconductor has been studied. This was accomplished by investigating the nuclear magnetic resonance of two groups of (type-I) superconducting samples. In the first group of samples, consisting of different-sized samples of pure lead, the residual NMR shift in the limit of zero temperature was found to vary with particle size, as is true for pure tin. The results are consistent with the existence of a larger spin-orbit interaction in lead. The second group of samples, containing various concentrations of In, Sb, Pb, and Bi impurities, exhibited residual NMR shifts which were consistent with the spin-orbit interactions characteristic of the respective impurities. Taken together, the NMR results are consistent with the microscopic theory of superconductivity, including the effects of spin-orbit interactions.

### I. INTRODUCTION

In the 13 years that have passed since the development of the Bardeen, Cooper, and Schrieffer (BCS) theory,<sup>1</sup> most of the properties of superconductors have been explained. Using the BCS description, Yosida<sup>2</sup> calculated the conduction-electron paramagnetic spin susceptibility as a function of temperature for a superconductor, and as a result of the pairing of electronic spins, he predicted a vanishing susceptibility at  $T = 0^\circ\text{K}$ . The electronic spin susceptibility may be investigated directly by measuring the shift of the nuclear magnetic resonance. For simple metals, the NMR shift has been attributed to the paramagnetism of the conduction-electron spins, together with their contact hyperfine interaction with the nucleus.<sup>3</sup> However, NMR experiments on various superconductors have shown a nonvanishing shift as the temperature is extrapolated to zero, in apparent disagreement with the theory.<sup>4-6</sup> Two general ideas have been proposed to explain the residual NMR shift in superconductors: (i) In a superconductor, the paramagnetic spin susceptibility (temperature dependent) is modified by spin-reversing

scattering due either to the boundaries of the small specimens or to the presence of impurities,<sup>7-9</sup> and (ii) there exist other contributions to the shift which are temperature independent in the superconducting state.<sup>10,11</sup> (It must be remembered that because of the Meissner effect, NMR experiments in type-I superconductors have required samples such that at least one dimension is the order of a few hundred angstroms.) Recent work by Wright<sup>12,13</sup> on tin particles, in which the electronic mean free path was limited by varying the particle size, supports the spin-reversing scattering theory. He found that the residual shift was a function of the particle size and that the data fit the spin-reversing scattering theory best by assuming that any other contributions (temperature independent in the superconducting state) were unimportant. However, because only the electronic mean free path is varied, Wright's experiments alone do not demonstrate conclusively the effect of the spin-orbit coupling. It is the purpose of the present work to illustrate the effect of the spin-orbit coupling strength on the spin-reversing scattering and hence the electronic spin susceptibility. This has been done in two ways by performing two series of experiments. In

the first series of experiments, samples (similar to Wright's tin samples) were made of another pure superconductor which had a different spin-orbit coupling. In particular, the residual NMR shift was measured in pure lead samples<sup>14</sup> of various particle sizes which were comparable to the tin samples in every respect except, of course, spin-orbit coupling. The results show that, although small-particle line broadening exists, the NMR for superconducting lead can be observed, and the residual shift is affected by the particle size as was the case for tin. The effect of the increased spin-orbit coupling of lead with respect to tin is apparent; i. e., an electron in a lead particle has a higher probability of having its spin flipped in a collision with the boundary than an electron in a tin particle. In the second series of experiments, impurities of various spin-orbit coupling strengths were added to a well-known superconductor (tin),<sup>12</sup> and the results were consistent with the spin-reversing scattering theory. In particular, NMR samples of tin containing up to 1-at. % Pb, Bi, In, or Sb impurity were constructed. Here, the electronic mean free path is varied by impurity concentration instead of particle size, and the probability for flipping an electron spin in a collision is determined by the spin-orbit coupling strength of the scattering center. It is found that adding a small amount of indium or antimony (weak spin-orbit coupling) has small effect on the residual shift, while the same amount of lead or bismuth (strong spin-orbit coupling) increases the residual shift significantly.

Experimental work by Hammond and Kelly<sup>15</sup> on pure 120-Å aluminum films shows no residual shift at  $T = 0^\circ\text{K}$ , which is to be expected since aluminum has a very small spin-orbit interaction (see also Ref. 16). We feel that our results, together with Hammond and Kelly's aluminum work, provide very strong evidence for the spin-orbit coupling and its effect on the electronic spin susceptibility of superconductors through spin-reversing scattering. In view of this, the apparent discrepancy between the BCS theory and NMR experiments in superconductors seems to be reconciled. The conclusions in this paper are applicable to type-I  $s$ - $p$  superconductors.

## II. THEORY

We will now briefly discuss the three principal papers on spin-reversing scattering theory.

### A. Spin-Reversing Scattering: Ferrell

The above spin-reversing scattering explanation of the residual shift in superconductors was first introduced by Ferrell.<sup>7</sup> Qualitatively, in the case of a pure small metallic particle, Ferrell obtains

(for  $fL < \xi_0$ )

$$K_S(0)/K_N = \chi_S(0)/\chi_N \approx 1 - fL/\xi_0, \quad (1)$$

where  $K_S(0)/K_N$  is the fraction of the normal-state shift (susceptibility) remaining in a superconductor at zero temperature,  $L$  is the radius of the small particle,  $\xi_0$  is the coherence length, and  $f$  is the number of times an electron scatters off the boundary of this particle before spin-orbit coupling flips its spin.

### B. Spin-Reversing Scattering: Anderson

In a more quantitative approach, Anderson<sup>8</sup> shows that when there is electronic scattering (from the boundaries of a small specimen or from impurities) in the presence of spin-orbit interaction, plane-wave states with fixed spin are no longer good one-electron wave functions ( $\vec{k}$  and  $\sigma$  are no longer good quantum numbers). Using his theory of "dirty" superconductors, Anderson introduces the hypothetical exact one-electron wave function  $\psi_n = \sum_{\vec{k}, \sigma} \langle n | \vec{k} \sigma \rangle \psi_{\vec{k}, \sigma}$  with energy  $E_n$ . In the absence of magnetic centers, the Kramers time-reversal degeneracy must be present, so that the time-reversed state  $\psi_{-n}$  is also an eigenstate of energy  $E_n$ . Anderson then shows that the pairing of a state with its time-reversed counterpart (i. e.,  $n$  and  $-n$ ) leads to a BCS state which has essentially the average energy gap of the bulk superconductor. Properties of superconductors which arise from the gap nature alone are still preserved in the treatment. Using the BCS formalism modified with the new wave functions, Anderson calculates the electronic spin susceptibility for a superconductor and shows that the result confirms Ferrell's qualitative predictions. He finds

$$\chi_S(0)/\chi_N \approx 1 - (2l_s/\pi\xi_0) \quad \text{when } l_s \ll 2\pi^2\xi_0 \quad (2)$$

and

$$\chi_S(0)/\chi_N \approx \pi\xi_0/6l_s \quad \text{when } l_s \gg 2\pi^2\xi_0, \quad (3)$$

where  $l_s$  is the spin mean free path. In the case where  $l_s \ll 2\pi^2\xi_0$ , given by Eq. (2), we can see that this is the same as Ferrell's result except for the constant factor  $2/\pi$ , if we make the identification  $l_s = fL$ .

### C. Spin-Reversing Scattering: Abrikosov and Gor'kov

Anderson's calculation (mentioned above) does not take into account the effect of spin-reversing scattering on the energy gap or on the density of states for quasiparticle excitations in a superconductor. However, Abrikosov and Gor'kov<sup>9</sup> take all the effects of scattering into account by using their Green's-function formalism for impure superconductors to calculate the electronic spin susceptibility.

In their calculations, however, they assume that the mean free path for ordinary electronic scattering,  $l_e$ , is much smaller than the spin mean free path  $l_s$ :

$$\frac{\chi_S(0)}{\chi_N} = 1 - \frac{1}{\rho_0} \left( \frac{\pi}{2} - \frac{\cosh^{-1}\rho_0}{(\rho_0^2 - 1)^{1/2}} \right), \quad \rho_0 > 1 \quad (4)$$

and

$$\frac{\chi_S(0)}{\chi_N} = 1 - \frac{1}{\rho_0} \left( \frac{\pi}{2} - \frac{\cos^{-1}\rho_0}{(1 - \rho_0^2)^{1/2}} \right), \quad \rho_0 < 1 \quad (5)$$

where  $\rho_0$  is a measure of the amount of spin-reversing scattering and is defined by  $\rho_0 = 2\pi\xi_0/3l_s$ . A plot of the above function is shown in Fig. 6 of Ref. 13. It can be seen from this diagram that in the case of small  $\rho_0$  (large  $l_s$ ), we obtain the Yosida<sup>2</sup> result of vanishing susceptibility. However, in the case of large  $\rho_0$  (small  $l_s$ ), the susceptibility for the superconducting state approaches the normal-state value. We will make use of the Abrikosov-Gor'kov formalism in Sec. IV.

#### D. Appel's Approximate Calculation for "f"

In the three theories discussed above, there is one variable which is determined by the particular sample. This is the net-spin mean free path  $l_s$ . Once it is known, the residual electronic spin susceptibility  $[\chi_S(0)/\chi_N]$  can be obtained from any of the above expressions. As discussed in Ferrell's treatment, Sec. II A, it is convenient to express  $l_s$  as some constant  $f$  times the electronic mean free path,  $l_s = fl_e$ . Physically,  $f$  represents the number of times an electron scatters per spin flip, or equivalently,  $1/f$  is the probability of an electron flipping its spin in a scattering process. Also,  $l_e$  is limited by the boundaries of the specimen or impurities and is inversely related to the residual resistivity. Appel<sup>11</sup> estimates  $f$  to be the order of  $(\Delta E/\lambda)^2$ , where  $\lambda$  is the average spin-orbit coupling energy and  $\Delta E$  is a typical band gap. The band structure and Fermi surface have been calculated for both metallic lead<sup>17,18</sup> and metallic tin<sup>19</sup> by using orthogonalized-plane-wave and pseudopotential methods. One can look at the  $E(\vec{k})$ -vs- $\vec{k}$  curves for these two metals in an attempt to get some quantitative measure for the size of  $\Delta E$ . The values for  $\lambda$  may be obtained in two ways. A very rough measure for the spin-orbit energy is provided by the splitting of the atomic spectra.<sup>20</sup> Also,  $\lambda$  can be approximated from the values listed by Herman, Kuglin, Cuff, and Kortum.<sup>21</sup> We consider Appel's approximate method to be very crude and probably useful to only an order of magnitude.

#### E. Temperature-Independent Contributions

Up to this point, we have considered the residual shift in superconductors as being due to the con-

duction-electron paramagnetic spin susceptibility (temperature dependent) as modified by spin-reversing scattering and acting through the contact hyperfine interaction with the nucleus. In his work on small tin particles, Wright<sup>12,13</sup> has claimed that other contributions to the shift, "which are unchanged through the superconducting transition," are unimportant ( $\sim 10\%$ ). However, we do not feel that these contributions should be forgotten, nor do we deny the possibility that they might be more important for other materials (particularly type-II superconductors). We will briefly mention the two principal contributions to the shift which are temperature independent in the superconducting state.

#### 1. Van Vleck Orbital Paramagnetism

Kubo and Obata<sup>22</sup> have pointed out, for metals with partly filled non-s bands, the orbital magnetic moment can contribute to the paramagnetic susceptibility through second-order perturbation. This contribution corresponds to the so-called "temperature-independent high-frequency term," or Van Vleck susceptibility of atoms, and is particularly important in transition metals where the 3d bands are partially filled. For Sn and Pb, we would be interested in the 5p and 6p electrons, respectively. Orgel<sup>23</sup> was the first to suggest that this Van Vleck-type orbital susceptibility would give rise to a shielding of the nuclear moment and contribute appreciably to the NMR shift. Clogston, Gossard, Jaccarino, and Yafet<sup>10</sup> and Noer and Knight<sup>6</sup> have discussed the possibility of this mechanism giving rise to the residual shift in superconductors, as it is expected to remain unchanged through the superconducting transition. This contribution to the shift would be independent of temperature and particle size.

#### 2. Crystalline-Field Spin-Orbit Coupling

Appel<sup>11</sup> claims that since the BCS theory is a nonrelativistic theory, spin-orbit coupling and other relativistic effects which arise from the periodic electric field of the crystal lattice are ignored. He calculates two contributions to the contact shift which are attributed to the spin-orbit coupling force of the periodic potential. First, in the presence of an external magnetic field, this force causes virtual transitions from (connects) the BCS ground state to excited states with energies  $>> 2\epsilon_0$  (energy gap) and produces a significant contribution to the spin susceptibility which is, like the paramagnetic orbital susceptibility of transition metals, temperature independent and of the type known as Van Vleck or high-frequency paramagnetism. This spin-orbit coupling effect is a bulk effect and involves only electrons near the Fermi surface. It is size independent and, therefore,

should be separable from the one caused by scattering of the electrons at impurities or boundaries.

Furthermore, in the presence of spin-orbit coupling, there is a second contribution to the contact shift which has no comparable part in the spin susceptibility. It arises from electrons inside the Fermi surface because of the interaction between the electron spin and orbital motion via spin-orbit coupling and the interaction between the orbital motion and magnetic field. In calculating the total Van Vleck-type contribution to the contact shift, Appel generalizes Wannier's formalism to a relativistic Bloch electron in a magnetic field. He finds that for the normal state  $K_c^{20}$ , the total spin-orbit contribution to the total contact shift  $K_c$ , has two terms (mentioned above) of the order  $\lambda/\Delta E$ , i. e.,

$$K_c^{20} \sim [\pm \alpha(\lambda/\Delta E) \pm \beta(\lambda/\Delta E)] K_c, \quad (6)$$

where  $\lambda$  is the average spin-orbit coupling energy,  $\Delta E$  is an average energy gap between conduction-band states and excited states to which the orbital angular momentum connects, while  $\alpha$  and  $\beta$  are constants the order of unity. There is an ambiguity in the signs for both terms. The first term is the contribution from electrons near the Fermi surface and is expected to be affected by the superconducting transition, while the second term represents the contribution from electrons inside the Fermi surface and remains unaffected by this transition. Gor'kov<sup>24</sup> claims that the first term in the above expression, which is the order of  $\lambda/\Delta E$  in the normal state for a metal, becomes the order of  $(\lambda/\Delta E)^2$  in the superconducting state and, therefore, is negligible. However, the second term still remains the order of  $\lambda/\Delta E$  and could possibly contribute to the residual shift for a superconductor, although there is still an ambiguity in the sign.

Wright<sup>12,13</sup> has designated these contributions as "unchanged through the superconducting transition"; however, this is really not a correct designation, as the first term in Appel's contribution does change through the transition. We prefer to use the designation "temperature independent in the superconducting state" for these contributions. If any of the above mechanisms have a significant contribution to the total shift, they must be subtracted before we can utilize the spin-reversing scattering formalism.

### III. APPARATUS AND EXPERIMENTAL PROCEDURES

#### A. Sample Preparation

##### 1. Construction of Alloys

NMR samples were made of pure tin, pure lead, and tin with various concentrations of In, Pb, Sb,

and Bi impurity. For the impurity samples, we had to be concerned with metallurgy problems in the preparation of the alloys, and a procedure described by Lee and Raynor<sup>25</sup> was followed to ensure homogeneity. A total of six 5-g ingots of binary tin-rich alloys were made: (A1) Sn + 1-at. % In, (A2) Sn +  $\frac{1}{2}$ -at. % Pb, (A3) Sn + 1-at. % Pb, (A4) Sn +  $\frac{1}{2}$ -at. % Sb, (A5) Sn +  $\frac{1}{2}$ -at. % Bi, and (A6) Sn + 1-at. % Bi. Tin was chosen as the host because its NMR had been studied quite extensively in the superconducting state.<sup>5,12,13</sup> Wright<sup>12,13</sup> has measured the residual shift as a function of the particle size and this information is needed if we are to determine independently what effect the addition of impurities has. In choosing the various types of impurities, we had to be concerned with their solid solubility in tin as well as their spin-orbit interaction. Phase diagrams are provided for these alloys by Hansen<sup>26</sup> and Elliott.<sup>27</sup> The various binary ingots (as well as pieces of pure tin and lead) were extruded into a wire with a diameter of 0.033 in. With the material in the form of a wire, we could then construct the nuclear resonance samples.

#### 2. Evaporation of Samples

Because of the Meissner effect, NMR experiments on superconducting metals have required samples with at least one dimension less than the penetration depth. Androes<sup>5</sup> (and later, Wright<sup>12,13</sup>) was able to produce small "platelets" of tin by vacuum evaporation, whose dimensions were small enough to overcome this problem. During the course of this work, it was discovered that, upon vacuum evaporation, lead<sup>14</sup> forms small particles in a similar manner. We employed the same technique to make our small-particle NMR samples. An evaporator, which was an improved version of the one described in detail by Androes, Hammond, and Knight,<sup>28</sup> was constructed, and we need only briefly discuss the interior of the system here. The extruded wire was loaded into a mechanism which chopped off equal bits (about 2 mm long) and allowed them to fall, via a retractable spout, into a tungsten boat for evaporation. The spout and chopping mechanism were controlled from outside the system, and any desired number of bits of the metal could be dropped into the boat. The metal was evaporated by passing a large current through the tungsten boat and a layer of small particles condensed on our substrate. The size of these particles was controlled by the amount of material evaporated and the rate of evaporation. A dielectric layer could be deposited over the metal particles by opening the shutter door of the SiO furnace. This SiO source, which is described by Drumheller,<sup>29</sup> ran continuously within an enclosure.

The dielectric layer served to encase and insulate a layer of particles and allowed us to build up several insulated layers (60–130) of metal particles on our substrate. This multiple-layer technique was necessary to ensure an adequate filling factor for the NMR samples. The furnace evaporation rate could be calibrated by using a crystal-controlled rate monitor, similar to the one described by Lins and Kuluk.<sup>30</sup> Our substrate consisted of 0.0025-in.-thick Mylar, which passed from one spool over a copper backing plate and was taken up on a second spool, in a manner analogous to photographic film in a camera. Shields were arranged such that only the portion of the Mylar over the backing plate (11×12 cm) was exposed to the sources. The take-up spool could be rotated from outside the system and, hence, more than one sample could be made during a single pump-down cycle. The substrate was held at room temperature.

During a single pump-down cycle, two initial electron-microscope samples were evaporated; then, a nuclear-resonance sample; and finally, two more electron-microscope samples. The electron-microscope samples consisted of a single layer of metal particles which had been sandwiched between two dielectric layers. An NMR sample had several alternating layers of metal particles and dielectric. All the tin NMR samples consisted of 60 insulated particle layers, while the lead NMR samples had from 100 to 130 layers. After each sample, whether it be an electron-microscope or a nuclear-resonance sample, the take-up spool was rotated a prescribed number of turns to ensure that a completely clean section of the Mylar substrate was exposed. Pressures of  $2 \times 10^{-7}$  mm Hg were obtainable in this vacuum system; however, during the actual evaporation procedure, the pressure ranged from 4 to  $6 \times 10^{-7}$  mm Hg.

The samples were removed and the four electron-microscope samples were mounted on grids for observation by a procedure which will be described in Sec. III B. The NMR sample was folded carefully several times and taped between two tin glass plates. The final dimensions of the completed resonance sample were  $12 \times 6 \times 5$  mm.

## B. Sample Analysis

### 1. Particle-Size Determination

Two methods were used to prepare the electron-microscope specimens for observation. For the tin group, a small square section ( $2 \times 2$  mm) was cut from the  $11 \times 12$ -cm sample and sandwiched between two electron-microscope grids. The Mylar was dissolved off by a three-to-one mixture of trifluoroacetic acid and methylene chloride. The two grids were separated, and the film which

remained on one of the grids was a layer of tin particles encased in SiO. For each NMR sample, there were four electron-microscope specimens (two before and two after). It was found, however, that the solvent reacted strongly with the lead particles, and washed them away leaving residual pits in the SiO. It became necessary to use an alternative method for preparing the lead-group electron-microscope specimens.<sup>31</sup> A small amount of sodium metaphosphate ( $\text{NaPO}_3 \cdot 12\text{H}_2\text{O}$ ) was evaporated first to provide a thin  $\text{NaPO}_3$  layer between the Mylar and the lead-particle electron-microscope sample. Since the  $\text{NaPO}_3$  layer is water soluble, large pieces of the film (lead particles encased in SiO) could be floated off the Mylar and scooped up by an electron-microscope grid held with a pair of tweezers.

The electron-microscope specimens were observed with a magnification of 80 000 times, and photographs were taken for particle-size analysis. Photographs were also taken of the electron diffraction pattern. For a particular NMR sample, the particle and diffraction photographs for all four of the related electron-microscope specimens were checked for consistency. Treating the particles as "platelets" of diameter  $d$  and thickness  $t$ , we followed the procedure described by Wright.<sup>13</sup>

The average particle diameter was determined by measuring the areas of all the particles in a given sector of a photograph, and a diameter was assigned to each particle by treating its area as a perfect circle. In nuclear resonance, each particle contributes according to the number of nuclei in it (i. e., its volume); however, it was appropriate to assign each particle the same average thickness regardless of the diameter.<sup>13</sup> Hence, we only needed to weight each particle diameter according to its areas. The average particle diameter for a particular sample was simply  $\bar{d} = \sum_i d_i A_i / \sum_i A_i$ , where  $d_i$  is the diameter and  $A_i$  is the cross-sectional area of a particular particle. In this analysis, it was possible to calculate  $\sigma$ , which is the fraction of the area covered with particles. This parameter was useful in the thickness calculation.

The thickness of the particles was obtained by a solid-angle calculation, in which we took a " $\cos^2\theta$ " distribution<sup>32</sup> for the flux of evaporated metal atoms and a sticking factor of unity. The thickness  $t$  was given by  $t = 3m_0 N / 2\pi\rho r^2\sigma$ , where  $m_0$  is the mass of one bit of wire,  $N$  is the number of bits evaporated per layer,  $\rho$  is the bulk density of the metal,  $r$  is the source-to-substrate distance, and  $\sigma$  is the fraction of the area covered by particles. This method of determining the thickness has been checked against two alternate methods.<sup>13,33</sup> After determining the above dimensions, we were able to calculate an average par-

ticle size. This was taken to be the geometric mean of the diameter squared and the thickness  $(\bar{d}^2 t)^{1/3}$

## 2. Impurity Analysis

The electron diffraction rings were measured carefully for (A3) Sn+1-at. % Pb in the tin group and (B2) pure lead in the lead group. Within the accuracy of the measurements, the measured rings matched the known values for tin and lead, respectively, from x-ray data.<sup>34</sup> The diffraction rings for the other samples in the two groups were compared visually with these.

Wright<sup>13</sup> had one wire and one NMR sample analyzed spectroscopically for unwanted impurities that may have been picked up in the extruding or chopping process. He found them to be free of such impurities. Since our procedures are identical in this phase, we did not feel it necessary to repeat this analysis.

A check on the homogeneity of our alloys was made by cutting off a segment from each end of the Sn+1-at. % Bi wire after it was extruded. Each segment of wire was chemically analyzed for the atomic ratio of Bi to Sn. The results indicate that the alloy was homogeneous. The part of the wire which was first to emerge from the extruder had essentially the same Bi-to-Sn ratio as the part of the wire which emerged last from the extruder. Also, both pieces had ratios very close to 1 at. % as we would expect.

The composition of one NMR sample (Sn+1-at. % Bi) was checked by semimicroquantitative analysis to ensure that none of the added impurity was lost in the evaporation process. This analysis was performed twice and the results indicated that only 8% of the Bi impurity was missing, and this is within the error of the analysis. Also, an early NMR sample (Sn+1-at. % Pb) was analyzed for the atomic ratio of Pb to Sn by x-ray fluorescence. Although this method is approximate, all of the Pb appeared to be present. We conclude that none of our impurity was lost in the evaporation process.

## C. Nuclear Magnetic Resonance

### 1. Electronics

The nuclear-magnetic-resonance equipment was conventional and consisted of a marginal oscillator, which was an improved version of one described earlier.<sup>35</sup> The output from the oscillator was fed to a lock-in detector, followed by the memory unit of a Varian Model No. C-1024 time-averaging computer. This is a multistorage device (1024 channels), which allows one to sweep through the resonance many times and add the results of each sweep.<sup>36</sup> The time-averaging computer provided

a ramp voltage which was put across a Varicap voltage-sensitive capacitor. This Varicap capacitor was in parallel with the marginal-oscillator-tuned circuit, and by varying the height of the ramp voltage, we selected the desired frequency sweep range. The frequency was measured by mixing the marginal-oscillator signal with that of a standard No. BC-221 rf generator and reading the beat frequency on a frequency meter. The NMR signal voltage could be read out of the computer directly onto the y axis of an xy recorder. The frequency meter provided a voltage which was linear with frequency, and this could be fed to the x axis of the recorder. The ramp voltage on the Varicap capacitor was not linear with the frequency and, hence, could not be used for this purpose.

### 2. Magnet

Fields up to 10 kG were available from a Varian Model No. V-2100 B regulated power supply and electromagnet. The magnetic field was measured in two ways. First, the absolute value of the field could be measured to an accuracy of  $\pm 2$  G with a rotating-coil gaussmeter, and second, a marginal-oscillator monitoring system was used to measure the stability of the field as well as the absolute value. The monitor probe contained a solution of Li<sup>7</sup> ions doped with paramagnetic Fe ions. The field was modulated at 154 Hz by an additional set of coils.

### 3. Cryogenics

The low temperatures required for these experiments were obtained by using a system of silvered-glass double Dewars. Temperatures in the range 4.2–1.4 °K were obtained by pumping on the helium bath with a mechanical pump through a Cartesian manostat. The temperature was measured by using mercury and oil manometers, which were calibrated with the  $T_{55E}$  helium-vapor-pressure curves.<sup>37</sup>

## IV. RESULTS AND DISCUSSION

### A. Tin with Impurities

#### 1. Nuclear Magnetic Resonance

For each sample of group A (tin group), at least two resonance lines were obtained at 4.2 °K and then, after pumping down, at least two more lines were obtained at 1.4 °K. The monitor checked the stability of the magnet and ensured that the field did not change during the run. A single resonance line consisted of 70 sweeps and took approximately 1 h to collect. The field was about 3800 G.

Our calculations are based on  $\alpha$  tin as the non-metallic reference,<sup>5,38</sup> which gives a value of 0.77% for the shift of the normal metal. This shift is 46.6

TABLE I. Tin-impurity data. Values in parentheses correspond to the residual shift for the pure tin sample (see Sec. IV).

Sample	$\chi_S/\chi_N$ (expt)	$\bar{d}$ (Å)	$t$ (Å)	Average particle dimension = $(\bar{d}^2 t)^{1/3}$
(A0) Pure tin	$0.66 \pm 0.02$	680	170	420 (390)
(A1) Sn + 1-at. % In	$0.68 \pm 0.02$	680	170	420 (390)
(A2) Sn + $\frac{1}{2}$ -at. % Pb	$0.76 \pm 0.02$	680	170	420 (390)
(A3) Sn + 1-at. % Pb	$0.80 \pm 0.02$	680	170	420 (390)
(A4) Sn + $\frac{1}{2}$ -at. % Sb	$0.71 \pm 0.02$	590	130	360
(A5) Sn + $\frac{1}{2}$ -at. % Bi	$0.71 \pm 0.02$	730	180	460
(A6) Sn + 1-at. % Bi	$0.78 \pm 0.02$	1200	180	620

kHz at 3800 G. Since the tin transition temperature is  $3.72^\circ\text{K}$ ,<sup>39</sup> the lines collected at  $4.2^\circ\text{K}$  are characteristic of the normal metal and are chosen as a normalization point. The lines at  $1.4^\circ\text{K}$ , which are characteristic of the superconducting tin, are shifted downward in frequency from the normal lines by an amount which we have measured. This gives us the residual shift value  $K_S/K_N$  at  $1.4^\circ\text{K}$ ; however, it is desirable to make two small corrections before the data can be analyzed. First, we desire the residual shift at  $0^\circ\text{K}$ , and this can be obtained by assuming the Yosida<sup>2</sup> form for the temperature dependence. At  $1.4^\circ\text{K}$ , the superconducting line has dropped 94% of the drop which would occur at  $0^\circ\text{K}$ , and we adjust each superconducting value downward an additional 6%. Second, we have to subtract any other contributions to the shift which are temperature independent in the superconducting state. Wright<sup>12,13</sup> has found a "best value" for this to be 10%, with the remainder of the shift being attributed to Pauli paramagnetism as modified by spin-reversing scattering. Table I lists each sample (column one), along with the corresponding measured value of the residual ( $T=0^\circ\text{K}$ ) spin susceptibility  $\chi_S/\chi_N$  (column two). The error limit on each value in column two is  $\pm 0.02$ .

### 2. Particle-Size Determination

Samples (A0), (A1), (A2), and (A3) were studied early in the course of the work. Comparing all of the electron-microscope specimens for these four samples showed them to have the same average particle dimension within the error of the measurement. It was believed that the addition of this small amount of impurity would have no effect on the dimensions of the resulting particles. As a result, the pure tin sample was selected as our normalization point, i. e., the average particle dimension, which had been assigned to these four samples, was the value which corresponds to the measured residual shift for the pure sample. Using Wright's<sup>12,13</sup> work, where the residual shift

for pure tin was determined as a function of the average particle dimension, our measured value of  $\chi_S/\chi_N = 0.66$  for sample (A0) corresponds to a particle size of  $390 \text{ \AA}$ . As a check of this result, one of the electron-microscope specimens was selected and a particle-size determination was made using the procedure described in Sec. III. The average particle dimension turned out to be  $420 \text{ \AA}$ , which compares very well with the above result.

As the work progressed and samples (A4), (A5), and (A6) were studied, it was found that the addition of the Sb and Bi impurity had a significant effect on the resulting particle size. It must be emphasized that for each of these three samples, the four corresponding electron-microscope specimens were consistent among themselves but differed from sample to sample. Also, additional electron-microscope specimens, which were made at a later time, compared favorably with the originals. Hence, these three samples cannot be normalized to some pure tin sample, and a particle-size determination was undertaken for each one.

The corresponding particle dimensions for each sample are listed in Table I. The average particle diameter  $\bar{d}$  and the particle thickness  $t$  are listed in columns three and four, respectively. These values are determined by the methods described in Sec. III. The average particle dimensions (geometric means) are listed in column five. For samples (A0), (A1), (A2), and (A3), the values in the parentheses, obtained in the manner described above, will be used in the actual analysis of the data (see Table I, column five).

### 3. Analysis of Data

In his work, Wright<sup>13</sup> takes the boundary-limited electronic mean free path  $l_{\text{ob}}$  for his pure tin particles as one-half the average particle dimension, or  $l_{\text{ob}} = \frac{1}{2}(\bar{d}^2 t)^{1/3}$ . The factor one-half is introduced in order to satisfy the limiting case of a sphere, where the mean free path is one-half the diameter. Wright shows a plot of the fraction of the normal-state shift remaining in the superconductor at zero temperature  $K_S(0)/K_N$ , as a function of  $l_{\text{ob}}$ . In Fig. 1, we reproduce this plot including additionally our own impurity data. The open circles and the curve represent Wright's pure tin data, while the solid circles are our data. The effect of various impurities in increasing the spin-reversing scattering and, hence, the residual shift is evident. It can be seen from Fig. 1 that adding 1 at. % of a material with weak spin-orbit coupling (e. g., In or Sb) has little effect on the residual shift, while 1 at. % of a material with strong spin-orbit coupling (e. g., Pb or Bi) increases the residual shift significantly.

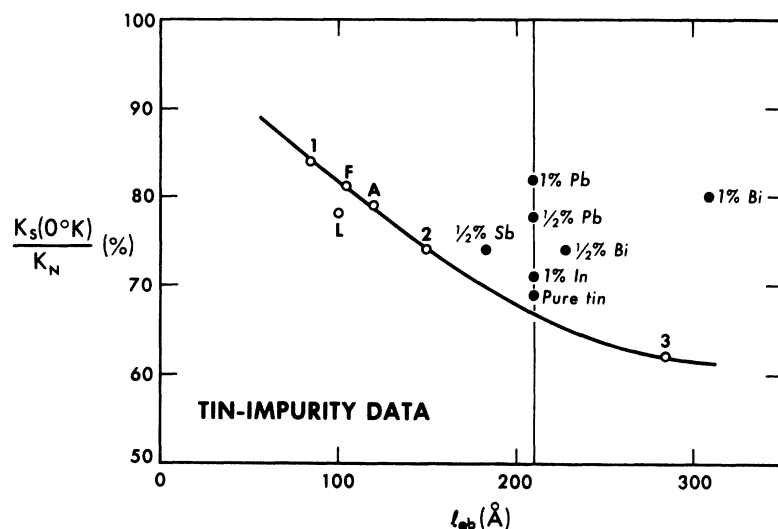


FIG. 1. Tin-impurity data. Residual NMR shift at zero temperature. The boundary-limited electronic mean free path,  $l_{ob} = \frac{1}{2}(td^2)^{1/3}$ .

In analyzing the results of this work, we must ask: "What is the net-spin mean free path  $l_s$ ?" In the case of the impurity samples, there are two scattering processes which limit the mean free path. First, as in the case of the pure tin work, the boundary scattering must be considered. Wright<sup>13</sup> takes the boundary-limited spin mean free path  $l_{sb}$  as being some constant times  $l_{ob}$  (i. e.,  $l_{sb} = f_b l_{ob}$ ). Physically, the constant  $f_b$  represents the number of times an electron scatters off of the boundary per spin flip. It is a measure of the spin-orbit interaction of the metal and should be independent of particle size. Wright found that  $f_b = 8$  for tin. Second, we have to consider the contribution of the impurity scattering. In the same manner, we take the impurity-limited spin mean free path  $l_{si}$  as being some constant times the impurity-limited electronic mean free path  $l_{ei}$  (i. e.,  $l_{si} = f_i l_{ei}$ ). Here,  $f_i$  represents the number of times an electron scatters off an impurity per spin flip. It is a measure of the spin-orbit interaction of the scattering center and should be independent of the impurity concentration. We will

be interested in comparing these  $f_i$ 's for the various impurities. The value of  $l_{si}$  can be derived from residual resistivity data. These two spin mean free paths add reciprocally to give  $l_s$  for the particular sample ( $1/l_s = 1/l_{sb} + 1/l_{si}$ ). In column one of Table II, we have listed the various impurity samples. In column two are listed the respective experimental values of  $\chi_S/\chi_N$ . The values of  $\rho_0$ , obtained from the experimental values of  $\chi_S/\chi_N$  by using the Abrikosov-Gor'kov plot, are listed in column three. In column four, we have used the definition of  $\rho_0$  ( $\rho_0 = 2\pi\xi_0/3l_s$ , where  $\xi_0 = 2000$  Å for tin)<sup>13</sup> to calculate  $l_s$ . In column five are listed the values for the boundary-limited spin mean free path which were obtained from  $l_{sb} = f_b l_{ob}$ , where  $f_b = 8$  (Wright's pure tin work) and  $l_{ob} = \frac{1}{2}(td^2)^{1/3}$  (see Table I, column five). The impurity-limited spin mean free paths, listed in column six, were obtained from  $1/l_{si} = 1/l_s - 1/l_{sb}$ . In column seven, we have listed the ratio of the residual resistivity of tin (for the particular impurity and concentration) at 0°K to that of tin at 273°K (taken from Aleksandrov<sup>40</sup>). It is conven-

TABLE II. Analysis of tin-impurity data.

Sample	$\chi_S/\chi_N$	$\rho_0$	$l_s$ (Å)	$l_{sb}$ (Å)	$l_{si}$ (Å)	$10^3 \frac{R_0}{R_{273}}$	Expt $(f_i)_{\text{impurity}}/(f_i)_{\text{Bi}}$	Calc $(f_i)_{\text{impurity}}/(f_i)_{\text{Bi}}$
(A0) Pure tin	0.66	2.7	1600	1600	$\infty$	0	...	...
(A1) Sn + 1-at. % In	0.68	3.0	1400	1600	14000	42.7	79	47
(A2) Sn + 1/2-at. % Pb	0.76	4.5	930	1600	2300	7.8	{ 2.4	{ 1.7
(A3) Sn + 1-at. % Pb	0.80	5.7	740	1600	1400	15.6	{ 2.9	{ 1.7
(A4) Sn + 1/2-at. % Sb	0.71	3.5	1200	1400	7500	28	28	10
(A5) Sn + 1/2-at. % Bi	0.71	3.5	1200	1800	3400	2.95	{ 1.3	{ 1.0
(A6) Sn + 1-at. % Bi	0.78	5.0	840	2500	1300	5.9	{ 1.0	{ 1.0



ient to express the  $f_i$ 's as ratios, where the particular  $f_i$  for the Sn+1-at. % Bi sample (since it produces the largest effect) is selected as the denominator. (Normalization with respect to Bi in this manner is convenient for computational purposes, as certain unknown quantities cancel in both the analysis of the experimental data and the theoretical estimates for the  $f_i$  values.) We use  $f_i = l_{\text{st}}/l_{\text{st}i}$ , where the values of  $l_{\text{st}}$  have been obtained experimentally (column six, Table II); and the  $l_{\text{st}i}$  are estimated from residual resistivity data<sup>40</sup> (column seven) by claiming that  $l_{\text{st}i} \propto (R_0/R_{273})^{-1}$ , since  $R_{273}$  is only a property of the tin host. It follows that  $f_i \propto l_{\text{st}}(R_0/R_{273})$ , and by taking ratios we can eliminate the constant of proportionality, giving

$$\frac{(f_i)_{\text{impurity}}}{(f_i)_{\text{Bi}}} = \frac{[l_{\text{st}}(R_0/R_{273})]_{\text{impurity}}}{[l_{\text{st}}(R_0/R_{273})]_{\text{Bi}}}$$

These values are listed in column eight of Table II.

We can now compare the values of  $(f_i)_{\text{impurity}} / (f_i)_{\text{Bi}}$  for the various impurities. These quantities are a measure of the strength of the spin-orbit coupling of the scattering center, i. e.,  $f_i$  is large for an impurity with weak spin-orbit coupling and small for an impurity with strong spin-orbit coupling. We find that In has the largest value of  $f_i$ , followed by Sb, Pb, and Bi. This is what we would expect from the size of the spin-orbit couplings for these particular impurities. The values connected by the curly bracket (column eight) should be the same, since they represent the same impurity and we expect the  $f_i$ 's to be independent of the concentration. In column nine, we have listed for comparison the values of  $(f_i)_{\text{impurity}} / (f_i)_{\text{Bi}} = (\lambda_{\text{Bi}}/\lambda_{\text{impurity}})^2$  calculated by Appel's approximate method.<sup>11,21</sup> We see that the agreement is quite good considering the crudeness of his method.

#### B. Pure Lead

##### 1. Nuclear Magnetic Resonance

Resonance lines for the samples of group B (lead group) were collected at  $T = 4.2^\circ\text{K}$  and  $T = 1.4^\circ\text{K}$ . One resonance line consisted of about 70 sweeps and took approximately 1 h to collect. The field used for the lead samples was about 6800 G.

Since the transition temperature for lead is  $7.18^\circ\text{K}$ ,<sup>39</sup> resonance lines collected at  $4.2$  and  $1.4^\circ\text{K}$  are characteristic of the superconducting metal. For some given field, these lines are shifted downward in frequency from where the normal-metal line would occur, with the  $1.4^\circ\text{K}$  line shifted downward slightly further than the  $4.2^\circ\text{K}$  line. In order to collect a normal line for a lead small-particle sample and use it as a ref-

erence point (as was done in the case of tin), it would be necessary to construct a heating device to use with the helium bath. This was not done in our lead experiments. Instead, we calculated the position of the salt and normal-metal lines by using a rotating-coil gaussmeter to measure the field and the accepted values for  $\gamma_{\text{salt}}^{\text{Pb}}$ <sup>41,42</sup> and the normal-state-metal shift<sup>43</sup> (0.8899 kHz G and 1.2%, respectively). At the above field, the normal-state shift is about 70 kHz. The measured values for the residual shifts in the superconducting samples are given in column five ( $4.2^\circ\text{K}$ ) and column six ( $1.4^\circ\text{K}$ ) of Table III. In the case of lead, where the transition temperature is high, the correction in the residual shift when extrapolating from  $1.4$  to  $0^\circ\text{K}$  is negligible. The "small-particle" broadening which occurred in Wright's<sup>12,13</sup> tin samples appeared to be more severe in the case of lead. The resonance line for sample (B1) was not observed; sample (B2) had a line which was barely usable, while for sample (B3) the line was by far the best, although still broad. The appropriate error limits are given for each value in columns five and six of Table III.

##### 2. Particle-Size Determination

A particle-size analysis, as described in Sec. III, was performed on each of the lead samples (see Table III, columns one through four).

##### 3. Analysis of Data

In analyzing the lead data, we cannot use the elaborate Abrikosov and Gor'kov spin-reversing scattering formalism because it requires that the spin mean free path  $l_s$  be much greater than the electronic mean free path  $l_e$ , and this is not satisfied for our lead particles because of the large spin-orbit interaction. Instead, we use Anderson's<sup>8</sup> approximate expression  $\chi_S/\chi_N \approx 1 - (2l_s/\pi\xi_0)$ , where  $\xi_0 = 830 \text{ \AA}$  for lead.<sup>44</sup> In the case of a pure sample,  $l_s$  is just equal to  $l_{\text{sb}}$ . Again, we take  $l_{\text{sb}} = f_b l_{\text{ob}}$ , where  $l_{\text{ob}} = \frac{1}{2}(\bar{d}^2 t)^{1/3}$ . Using the experimentally measured values of  $\chi_S/\chi_N$  [here,  $\chi_S/\chi_N = K_S(0)/K_N$ ] for each particle size, we calculate the corresponding  $f_b$  values. For sample (B2),  $f_b = 1.6$ , while sample (B3) gives  $f_b = 2.5$ .

TABLE III. Pure lead data.

Sample	$\bar{d}$ (Å)	$t$ (Å)	Average particle dimension $(\bar{d}^2 t)^{1/3}$	$K_S(4.2^\circ\text{K})/K_N$	$K_S(1.4^\circ\text{K})/K_N$
(B1) Pure lead	130	110	120	a	a
(B2) Pure lead	340	170	270	b	$0.83 \pm 0.06$
(B3) Pure lead	550	230	410	$0.67 \pm 0.04$	$0.60 \pm 0.04$

<sup>a</sup>No resonance line observed.

<sup>b</sup>Resonance line observed, but not usable.

In the above calculations, we assumed that all of the residual NMR shift is due to spin-reversing scattering. By subtracting various amounts of the residual shift (as would be necessary if there existed contributions other than spin-reversing scattering), there was no improvement in the consistency of the  $f_b$  values. For tin, Wright<sup>12,13</sup> found that the best fit was obtained by taking spin-reversing scattering as dominant (about 90%) and  $f_b = 8$ . In our lead particles  $f_b$  appears to be  $\approx 2$ , which is to be expected since lead has a larger spin-orbit interaction than tin.

At this point, we feel it necessary to elaborate on the possible existence of temperature-independent contributions to the total shift in our lead samples. Above, in our calculations for  $f_b$ , we attribute all of the shift to Pauli paramagnetism, which is modified by spin-reversing scattering in the superconducting state. However, it is entirely possible that the contributions to the shift which are temperature independent in the superconducting state (discussed at the end of Sec. II) could account for 0 to 30% of the total shift. Because of the magnitude of the size effect in lead, we feel that spin-reversing scattering provides the major contribution to the residual shift (as was the case in tin), and it is unlikely that the above-mentioned contributions are greater than  $\pm 30\%$ . Since we are unable to utilize the elaborate Abrikosov-Gor'kov theory and the data are limited, we cannot make as good an estimate for the temperature-independent contributions in our pure lead samples as Wright did for pure tin. However, our calculated values of  $f_b$  are not greatly affected by attributing up to  $\pm 30\%$  of the total shift to the temperature-independent contributions. By subtracting from the residual shift, constant contributions in this range ( $-30\%$  to  $+30\%$ ), the  $f_b$  values calculated with Anderson's expression varied from 1.3 to 3.0. These values are still significantly smaller than the value of  $f_b = 8$  for tin. Although the temperature-independent contributions do not appear to be as important as the spin-reversing scattering contribution for these two metals (and probably other type-I superconductors), we certainly cannot claim that they are completely negligible, particularly in the case of lead. The temperature-independent contributions actually appear to dominate in type-II superconductors.

#### V. CONCLUSIONS

It was the purpose of this work to illustrate the effect of the spin-orbit coupling strength on spin-reversing scattering and hence the residual electronic spin susceptibility and NMR shift of superconductors. This has been done in two ways by performing NMR experiments on two groups of samples. The results for the pure lead group in-

dicating the following: (i) Although small-particle line broadening exists, the NMR for superconducting lead can be observed; (ii) the residual shift is affected by the particle size as was the case for pure tin<sup>12,13</sup>; and (iii) the effect of the increased spin-orbit coupling of lead with respect to tin is apparent, i. e., an electron in a lead particle has a higher probability of having its spin flipped in a collision with the boundary than an electron in a tin particle. Experiments by Hammond and Kelly<sup>15</sup> on 120-Å aluminum films show no residual shift at  $T = 0^\circ\text{K}$ , which is to be expected since aluminum has a very small spin-orbit interaction (Yosida<sup>2</sup> limit). (Some recent work by Fine, Lipsicas, and Strongin<sup>16</sup> on aluminum films also shows a vanishing residual shift.) The results for the dilute tin-alloy group are consistent with the above results. Here, the electronic mean free path is varied by impurity concentration instead of particle size, and the spin-orbit coupling of the scattering center is important. Adding a small amount of an impurity with weak spin-orbit coupling has little effect on the residual shift, while adding the same amount of an impurity with strong spin-orbit coupling increases the residual shift significantly. We conclude that our results, together with the work of Hammond and Kelly and the aluminum work of Fine *et al.*, provide very strong evidence for the effect of spin-orbit coupling on the electronic spin susceptibility of superconductors through spin reversing. In view of this, the apparent discrepancy between the BCS theory and NMR shift experiments in superconductors seems to be reconciled.

#### ACKNOWLEDGMENTS

The authors would like to acknowledge several people who have contributed to this research project. Above all, we wish to thank Dr. Fulton Wright for his assistance in the early phases of the project. Professor Ralph R. Hultgren and George Gordon were extremely helpful in problems involving metallurgy and x-ray analysis. Special thanks are due to Dr. Charles Koch and Thomas Morrison for spending considerable time in analyzing the samples. Also, we would like to acknowledge Dr. James H. McAlear and Phillip Lintilhac for their assistance with the electron microscope. The services of the Physics Department machine, glass, electronics, and student shops were of enormous value throughout the course of this work. Special thanks go to Eric W. Peterson of the machine shop for his skill during the construction of the new evaporator. Finally, it is our pleasure to acknowledge several stimulating discussions with Dr. Joachim Appel, Dr. Robert H. Hammond, Professor J. Woods Halley, Professor Leo Brewer, and Professor Charles Kittel.

\*Work based in part upon a Ph. D thesis by W. A. Hines at the University of California at Berkeley, 1967; work supported in part by the U. S. Office of Naval Research.

†Present address: Department of Physics and Institute of Materials Science, University of Connecticut, Storrs, Conn. 06268

- <sup>1</sup>J. Bardeen, L. N. Cooper, and J. R. Schrieffer, *Phys. Rev.* **108**, 1175 (1957).  
<sup>2</sup>K. Yosida, *Phys. Rev.* **110**, 769 (1958).  
<sup>3</sup>C. H. Townes, C. Herring, and W. D. Knight, *Phys. Rev.* **77**, 852 (1950).  
<sup>4</sup>F. Reif, *Phys. Rev.* **106**, 208 (1957).  
<sup>5</sup>G. M. Androes and W. D. Knight, *Phys. Rev.* **121**, 779 (1961).  
<sup>6</sup>R. J. Noer and W. D. Knight, *Rev. Mod. Phys.* **36**, 177 (1964).  
<sup>7</sup>R. A. Ferrell, *Phys. Rev. Letters* **3**, 262 (1959).  
<sup>8</sup>P. W. Anderson, *Phys. Rev. Letters* **3**, 325 (1959).  
<sup>9</sup>A. A. Abrikosov and L. P. Gor'kov, *Zh. Eksperim. i Teor. Fiz.* **42**, 1088 (1962) [*Sov. Phys. JETP* **15**, 752 (1962)].  
<sup>10</sup>A. M. Clogston, A. C. Gossard, V. Jaccarino, and Y. Yafet, *Rev. Mod. Phys.* **36**, 170 (1964).  
<sup>11</sup>J. Appel, *Phys. Rev.* **139**, A1536 (1965).  
<sup>12</sup>F. Wright, W. A. Hines, and W. D. Knight, *Phys. Rev. Letters* **18**, 115 (1967).  
<sup>13</sup>F. Wright, *Phys. Rev.* **163**, 420 (1967).  
<sup>14</sup>W. A. Hines and W. D. Knight, *Phys. Rev. Letters* **18**, 341 (1967).  
<sup>15</sup>R. H. Hammond and G. M. Kelly, *Phys. Rev. Letters* **18**, 156 (1967).  
<sup>16</sup>H. L. Fine, M. Lipsicas, and M. Strongin (private communication).  
<sup>17</sup>J. R. Anderson and A. V. Gold, *Phys. Rev.* **139**, A1459 (1965).  
<sup>18</sup>T. L. Loucks, *Phys. Rev. Letters* **14**, 1072 (1965).  
<sup>19</sup>G. Weisz, *Phys. Rev.* **149**, 504 (1966).  
<sup>20</sup>C. E. Moore, *Atomic Energy Levels*, Natl. Bur. Std. Circular No. 467 (U. S. GPO, Washington, D. C., 1949).  
<sup>21</sup>F. Herman, C. D. Kuglin, K. F. Cuff, and R. L. Kortum, *Phys. Rev. Letters* **11**, 541 (1963).  
<sup>22</sup>R. Kubo and Y. Obata, *J. Phys. Soc. Japan* **11**, 547

(1956).

- <sup>23</sup>L. E. Orgel, *J. Phys. Chem. Solids* **21**, 123 (1961).  
<sup>24</sup>L. P. Gor'kov, *Zh. Eksperim. i Teor. Fiz.* **48**, 1772 (1965) [*Sov. Phys. JETP* **21**, 1186 (1965)].  
<sup>25</sup>J. A. Lee and G. V. Raynor, *Proc. Phys. Soc. (London)* **67B**, 737 (1954).  
<sup>26</sup>M. Hansen, *Constitution of Binary Alloys*, 2nd ed. (McGraw-Hill, New York, 1958).  
<sup>27</sup>R. P. Elliott, *Constitution of Binary Alloys, First Supplement* (McGraw-Hill, New York, 1965).  
<sup>28</sup>G. M. Androes, R. H. Hammond, and W. D. Knight, *Rev. Sci. Instr.* **32**, 251 (1961).  
<sup>29</sup>C. E. Drumheller, in *Proceedings of the Seventh National Symposium on Vacuum Technology*, 1961, p. 306 (unpublished).  
<sup>30</sup>S. J. Lins and H. S. Kuluk, in Ref. 29, p. 333.  
<sup>31</sup>Y. Iguchi, *Sci. Light (Tokyo)* **13**, 37 (1964).  
<sup>32</sup>L. Holland, *Vacuum Deposition of Thin Films* (Wiley, New York, 1966), p. 141.  
<sup>33</sup>W. A. Hines, Ph.D. thesis (University of California, Berkeley, 1967) (unpublished).  
<sup>34</sup>J. V. Smith, *Index (Inorganic) to the Powder Diffraction File*, ASTM No. PD1S-15i (American Society for Testing and Materials, Philadelphia, 1965).  
<sup>35</sup>R. V. Pound and W. D. Knight, *Rev. Sci. Instr.* **21**, 219 (1950).  
<sup>36</sup>M. P. Klein and G. W. Barton, *Rev. Sci. Instr.* **34**, 754 (1963).  
<sup>37</sup>J. R. Clement, *Phys. Rev.* **100**, 743 (1955).  
<sup>38</sup>N. Bloembergen and T. J. Rowland, *Acta Met.* **1**, 731 (1953).  
<sup>39</sup>P. G. de Gennes, *Superconductivity of Metals and Alloys* (Benjamin, New York, 1964), p. 17.  
<sup>40</sup>B. N. Aleksandrov, *Fiz. Metal. i Metalloved.* **14**, 434 (1962) [*Phys. Metals and Metallog. (USSR)* **14**, 96 (1962)].  
<sup>41</sup>*NMR Table*, 4th ed. (Varian Association, New Rochelle, N. Y., 1964).  
<sup>42</sup>T. J. Rowland, *Progr. Mater. Sci.* **9**, 1 (1961).  
<sup>43</sup>L. H. Piette and H. E. Weaver, *J. Chem. Phys.* **28**, 735 (1958).  
<sup>44</sup>P. G. de Gennes, in Ref. 39, p. 24.